J. Ocean Univ. China (Oceanic and Coastal Sea Research)
https://doi.org/10.1007/s11802-019-4018-z
ISSN 1672-5182, 2019 18 (5): 1051-1060
http://www.ouc.edu.cn/xbywb/
E-mail:xbywb@ouc.edu.cn

The Performance of Dual-Frequency Polarimetric Scatterometer in Sea Surface Wind Retrieval

LIU Shubo[1), 2), *], WEI Enbo[3), *], JIN Xu[1)], LV Ailing[1), 2)], and DANG Hongxing[1)]

1) *Xi'an Institute of Space Radio Technology*, *China Academy of Space Technology*, *Xi'an* 710100, *China*
2) *National Key Laboratory of Science and Technology on Space Microwave*, *Xi'an* 710100, *China*
3) *Institute of Oceanology and Center for Ocean Mega-Science*, *Chinese Academy of Sciences*, *and Qingdao National Laboratory for Marine Science and Technology*, *Qingdao* 266071, *China*

(Received October 12, 2018; revised November 28, 2018; accepted January 7, 2019)

Abstract The wind retrieval performance of HY-2A scanning scatterometer operating at Ku-band in HH and VV polarizations has been well evaluated in the wind speed range of 0–25 m s^{-1}. In order to obtain more accurate ocean wind field, a potential extension of dual-frequency (C-band and Ku-band) polarimetric measurements is investigated for both low and very high wind speeds, from 5 to 45 m s^{-1}. Based on the geophysical model functions of C-band and Ku-band, the simulation results show that the polarimetric measurements of Ku-band can improve the wind vector retrieval over the entire scatterometer swath, especially in nadir area, with the wind direction root-mean-square error (RMSE) less than 12° in the wind speed range of 5–25 m s^{-1}. Furthermore, the results also show that C-band cross-polarization plays a very important role in improving the wind speed retrieval, with the wind speed retrieval accuracy better than 2 m s^{-1} for all wind conditions (0–45 m s^{-1}). For extreme winds, the C-band HH backscatter coefficients modeled by CMOD5.N(H) and the ocean co-polarization ratio model at large incidence are used to retrieve sea surface wind vector. This result reveals that there is a big decrease of wind direction retrieval RMSE for extreme wind fields, and the retrieved result of C-band HH polarization is nearly the same as that of C-band VV polarization for low-to-high wind speed (5–25 m s^{-1}). Thus, to improve the wind retrieval for all wind conditions, the dual-frequency polarimetric scatterometer with C-band and Ku-band horizontal polarization in inner beam, and C-band horizontal and Ku-band vertical polarization in outer beam, can be used to measure ocean winds. This study will contribute to the wind retrieval with merged satellites data and the future spaceborne scatterometer.

Key words dual-frequency; polarimetric scatterometer; wind vector retrieval

1 Introduction

The observation of sea surface wind is essential to operate weather forecasting, shipping safety, hurricane and extra-tropical cyclone monitoring (Chelton and Xie, 2010; Wentz and Ricciardulli, 2011; Kasaka, 2014; Chiara, 2017). Radar scatterometer is designed to measure the sea surface wind field in terms of the normalized radar cross section σ_0 of the sea surface. The sea surface wind vector can be achieved by a series of processing stages including calibration, retrieving, and ambiguity removal (Schultz, 1990; Nghiem *et al.*, 1996; Stoffelen and Portabella, 2006; Lin *et al.*, 2017). Many satellite scatterometers had been launched for measuring the ocean wind vectors (Freilich *et al.*, 1994; Graf *et al.*, 1995; Freilich and Dunbar, 1999; Figa-Saldana *et al.*, 2002; Jayaram *et al.*, 2017; Durden and Perkovic-Martin, 2017), such as the National Aeronautics and Space Administration (NASA) scatterometer (NSCAT), the NASA SeaWinds scatterometer on QuikSCAT, the Advanced Wind Scatterometer (ASCAT) of European Meteorological Satellites and the China HY-2A scatterometer. These spaceborne scatterometers were designed at either Ku-band or C-band with co-polarization (HH or VV). Ku-band has the advantage of low wind speed measurement, and can enhance higher space resolution, while C-band is less affected by rain, water vapor and cloud liquid water in atmosphere. At present, the root-mean-square errors (RMSE) of 2 m s^{-1} and 20° have been reported for the wind speed and the wind direction retrieval accuracy with either C-band or Ku-band scatterometer, respectively.

A key remaining deficiency of current spacecraft scatterometers is their incapability to make unambiguous detection of wind direction. The SeaWinds and HY-2A scatterometers deployed a conical scanning antenna with inner and outer beams to achieve measurements from one to four azimuth directions at one wind vector cell (WVC) (Spencer *et al.*, 1997). The multiple azimuth measurements are helpful for determining the wind direction among several possible wind direction solutions. However, the wind retrieval in the inner and outer swath still suffer some degradation due to the separation of azimuth angles near

* Corresponding authors. E-mail: liushubo163@163.com
E-mail: ebwei@qdio.ac.cn

0° and 180° limiting the accuracy of retrieved wind direction. To deal with the ambiguity of wind direction retrievals, auxiliary wind field data or numerical weather model products are applied as a priori information to select the most likely value as a solution. However, relying on external information to improve scatterometer wind direction performance makes the retrieval process complicated.

In order to discuss the properties of radar scatterometer data varying with wind vector, both experiments and theoretical analysis have showed that the polarimetric scatterometer has the ability of enhancing the wind retrieval accuracy by simultaneously measuring conventional co-polarized backscatter and the polarimetric correlation of the co- and cross-polarized radar returns (Yueh *et al.*, 1994, 2002; Yueh, 1997; Tsai *et al.*, 2000). The co-polarized measurements are even-symmetric with respect to the wind direction, while the correlation between the co- and cross-polarized backscatter from sea surface has an odd-symmetry. The different symmetry properties between the copolarization and polarimetric correlation signatures indicate the ability of resolving wind direction ambiguity, and then enhance the overall wind retrieval performance across entire scatterometer swath.

Besides, several reports had qualitatively discussed the dual-frequency scatterometer with co-polarized measurements to improve spatial resolution and product quality of wind field (Gaston and Rodriguez, 2008; Rodriguez *et al.*, 2009). In this paper, we introduce the dual-frequency and polarimetric scatterometer, which can obtain more information of sea surface to quantitively analyze the performance of wind field retrieval by means of several simulation experiments from low to high wind speeds. It is expected that this simulation will make a better accuracy in retrieving wind vector comparing with conventional single frequency system. In Section 2 we introduce the geophysical model functions (GMFs) to simulate the sea surface wind retrieval. A brief description of simulation experiments is given in Section 3. In Section 4, the simulation results are given and discussed. Conclusions with recommendations are presented in Section 5.

2 Geophysical Model Function

GMF is the foundation of retrieving ocean wind vector from scatterometer measurements σ^0, where the scatterometer measurements and the polarimetric backscatter coefficients are related to the sea surface wind. The expression of GMF is usually derived from the comparison between actual backscatter measurements and a reference sea surface wind vector coming from independent observations or numerical model analyses in the form of

$$\sigma^0_{\mathrm{GMF}} = \mathrm{GMF}(ws, \varphi, p, f, \theta)\,, \tag{1}$$

where ws, φ, p, f and θ are wind speed, wind azimuth direction relative to the antenna beam look, polarization, microwave frequency and incidence angle, respectively. To retrieve low and high wind speed, we require both Ku-band and C-band GMFs of co- and cross-polarization, and the polarimetric backscattering coefficients. In addition, the valid domain of GMFs is defined as the wind speed range of 0–45 $\mathrm{m\,s^{-1}}$.

2.1 Ku-Band

2.1.1 Co-polarized GMF of Ku-band

The GMF of Ku-band has been developed over the past two decades (Linwood-Jones *et al.*, 1982; Freilich and Wentz, 1997; Wentz and Smith, 1999; Yueh *et al.*, 2001) although there still are some uncertainties of wind vector retrieval under the low and high wind conditions (Carswell *et al.*, 1994; Gaston and Rodriguez, 2008). The co-polarized GMF of HH and VV polarizations selected in this paper is the NSCAT-2 model (Wentz *et al.*, 1998) which was derived from NSCAT measurements and spatially and temporally collocated Numerical Weather Prediction (NWP) winds, and adopted for the final reprocessing of the entire mission of NSCAT. The NSCAT-2 model function of incidence angle 41° and 48° are shown in Figs.1(a) and (b) for the HH and VV polarizations of Ku-band, respectively. This GMF is an even function of relative azimuth angles, and expressed as follow:

$$\sigma^0_{\mathrm{PP}} = A_0 + A_1\cos(\varphi) + A_2\cos(2\varphi)\,, \tag{2}$$

where PP=HH/VV represents polarization, HH for horizontal polarization and VV for the vertical polarization. φ is the relative wind direction. A_0, A_1 and A_2 are coefficients which depend on the incidence angle, polarization and wind speed.

Unfortunately, NSCAT-2 is not valid for wind speed larger than 25 $\mathrm{m\,s^{-1}}$ since the most wind data used to develop NSCAT-2 are less than 25 $\mathrm{m\,s^{-1}}$. For winds lager than 25 $\mathrm{m\,s^{-1}}$, a new GMF of Ku-band was developed from the Imaging Wind and Rain Airborne Profiler (IWRAP) experiment of ocean backscatter observations for the ocean winds ranging from 25 to 65 $\mathrm{m\,s^{-1}}$ (Fernandez *et al.*, 2006). The GMF with the similar form of Eq. (2) provides an accurate relationship between σ^0 and the wind vector in the case of high wind speed. Figs.1(c) and (d) show the IWRAP-GMF function ranging from 25 to 50 $\mathrm{m\,s^{-1}}$ with a step of 5 $\mathrm{m\,s^{-1}}$ for HH and VV polarizations. It is seen that the backscatter coefficient tends to be saturate as the wind speed increases up to 50 $\mathrm{m\,s^{-1}}$, and the backscatter coefficients are symmetric with respect to the wind direction.

2.1.2 Cross-polarization GMF of Ku-band

Aircraft experiments and scattering theory indicate that cross-polarized backscatter has the similar directional information to co-polarized backscatter, but the mean value of cross-polarized backscatter coefficients is much smaller than that of copolarized backscatter at the same wind (Nghiem *et al.*, 1995; Moore and Fung, 1997). Up to now, few model functions of cross-polarization backscattering coefficients have been formally developed due to the sparsity of experimental data. Considering the small contributions of cross-polarized measurements to retrieve the ocean wind vector, we in this paper do not take the impact

of cross-polarizations of Ku-band on the wind retrieval into account.

2.1.3 Polarimetric GMF of Ku-band

Based on theoretical analysis, a parametric formulation of polarimetric model function was derived by Tsai (Tsai *et al*., 2000) for the wind speed less than 25 m s^{-1}. Their study showed that the polarimetric measurements are advantageous even though the magnitude of polarimetric signature is much lower than that of co-polarized backscatter coefficient. The complete Polarimetric GMF (PGMF) expression is given in the form (Tsai *et al.*, 2000)

$$\sigma^0_{\mu\theta\tau k} = a_1 \sin(\varphi) + a_2 \sin(2\varphi)\,, \tag{3}$$

where μ, θ, τ, k are either H or V. In this paper, μθτk is VHHH for inner beam and HVVV for outer beam. a_1 and a_2 are coefficients which depend on the wind speed and the incidence angle.

Plots of PGMF of Ku-band for HH and VV polarization are given in Figs.1(e) and (f). It is obvious that the polarimetric backscattering coefficient is odd-symmetric about the wind direction. However, there is few valid PGMF for wind speed lager than 25 m s^{-1}. Therefore, the polarimetric measurement is not considered in the simulation experiment for high wind speeds.

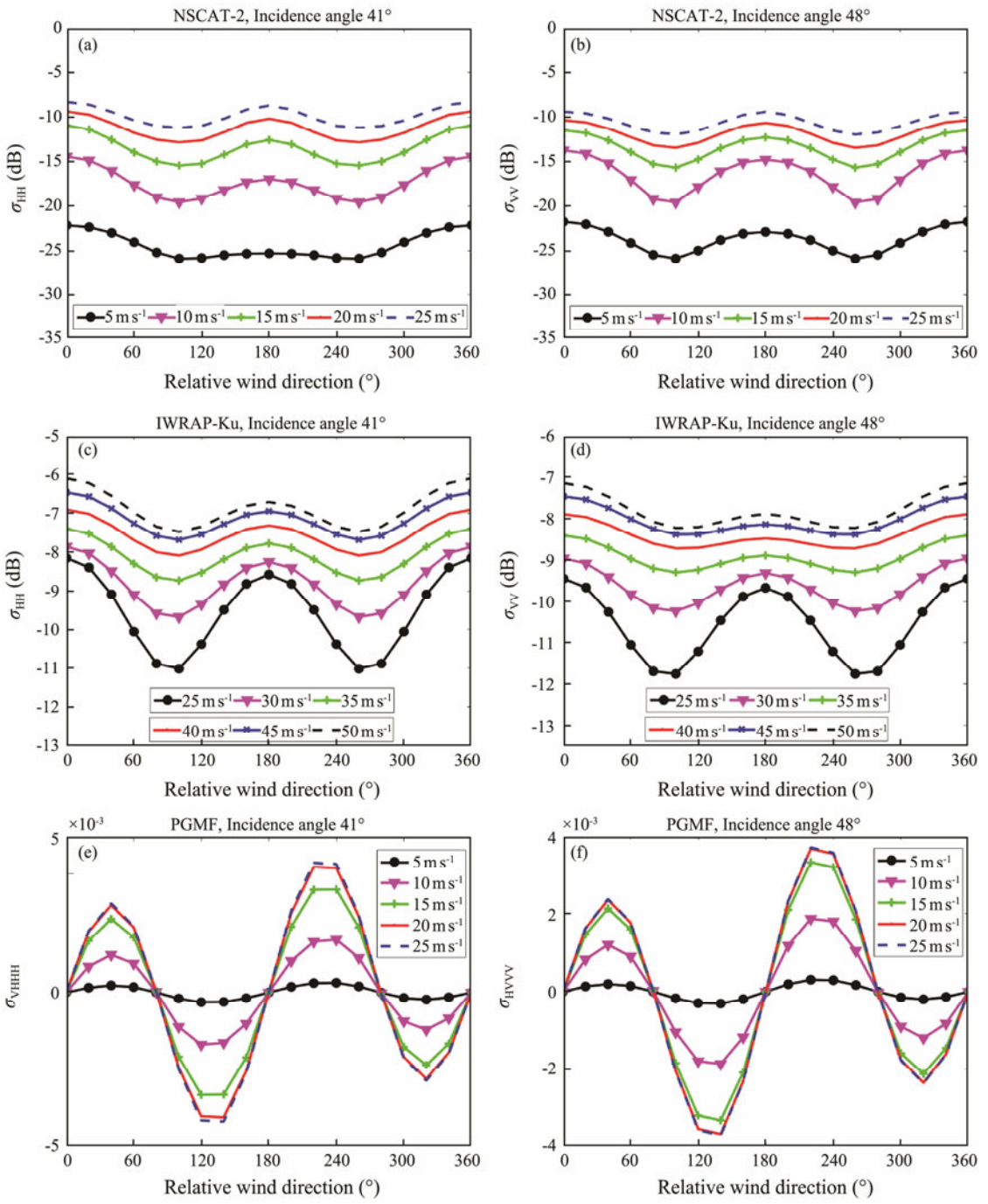

Fig.1 Plots of Ku-band geophysical model function for inner and outer beam. (a) NSCAT-2, HH; (b) NSCAT-2, VV; (c) IWRAP-KU, HH; (d) IWRAP-KU, VV; (e) PGMF, VHHH; (f) PGMF, HVVV.

2.2 C-Band

2.2.1 Co-polarized GMF of C-band

The GMF CMOD5.N (Hersbach, 2008; Verspeek *et al*., 2010) for vertically polarized backscatter was adopted to simulate the observed backscatter coefficients and to retrieve the ocean wind vector. It shows a good performance for the wind speed less than 25 m s^{-1}. However, the comparison of ASCAT measurements σ^0 with the retrieved wind vector of QuikSCAT reveals that ASCAT σ^0 still exhibits some sensitivities to wind speed, which are not found in the CMOD5.N GMF at higher wind speed (Soisuvarn *et al.*, 2008). Thus, for the wind speeds larger than 25 m s^{-1}, the CMOD5.H GMF model (Soisuvarn *et al*., 2013) developed by the aircraft-based scatterometer measurements, is used. The GMF of CMOD5.N and CMOD5.H were given by Hersbach (2008) and Soisuvarn *et al*. (2013) with similar form of Eq. (2).

The GMF of HH polarization was obtained by means of the ocean co-polarization ratio (*CPR)*,

$$\sigma^0_{\mathrm{HH}} = (1/CPR)\times\sigma^0_{\mathrm{VV}}, \tag{4}$$

where σ^0_{VV} is the vertically polarized ocean backscatter obtained from CMOD5.N. Plots of CMOD5.N and CMOD5.H for HH and VV polarizations are shown in Figs. 2(a), (b) and Figs.2(c) and (d), respectively. The ocean *CPR* used in Eq. (4) was obtained with the measurements of σ^0_{VV} and σ^0_{HH} from the airborne STORM data set at low winds and low incidences, and the airborne IWRAP data set at high winds and large incidences. The complete functional form of ocean CPR was given by Rivas *et al.* (2012).

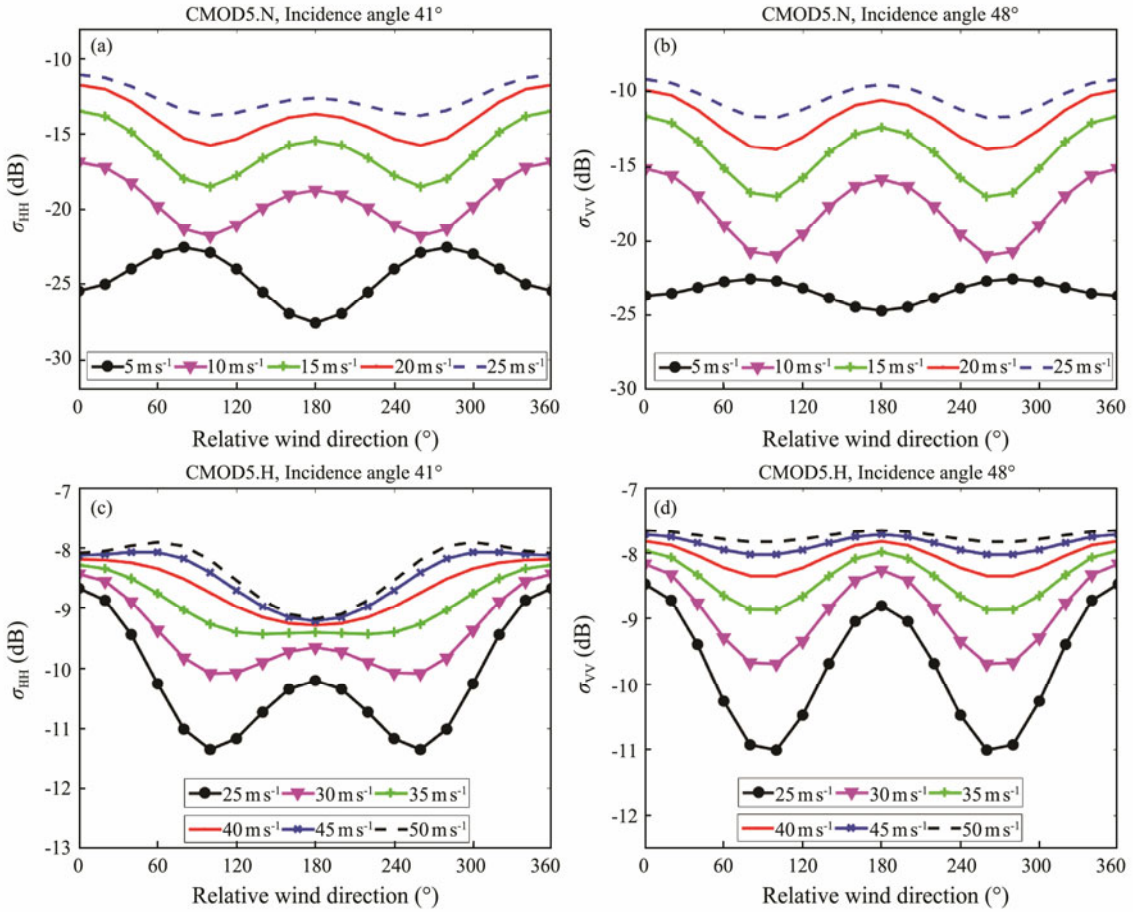

Fig.2 Plots of C-band geophysical model function. (a) CMOD5.N, HH; (b) CMOD5.N, VV; (c) CMOD5.H, HH; (d) CMOD5.H, VV.

2.2.2 Cross-polarized GMF of C-band

The cross-polarized GMF of C-band is developed with cross-polarized RADASAT-2 data (Hwang *et al.*, 2010; Vachon and Wolfe, 2011) for wind speed lower than 20 m s^{-1} and higher than 20 m s^{-1}, respectively. The two models show that the cross-polarized backscatter depends very weakly on the incidence angle and the wind direction, but strongly on wind speed. This indicates that the cross-polarization backscatters are very helpful for retrieving wind speed without a prior wind direction (Rivas *et al*., 2014). In addition, it can be inferred from the analysis of cross-polarizations that the backscatter coefficients of VH and HV polarizations are almost the same. The cross-polarized GMF is expressed as a function of wind speed as follows:

$$\sigma^0_{\text{cross-pol}} = 0.592\times Ws_{10} - 35.6,\ Ws_{10} < 20\ \mathrm{m\,s^{-1}}, \tag{5}$$

$$\sigma^0_{\text{cross-pol}} = 0.218 \times Ws_{10} - 29.1,\ Ws_{10} > 20\,\text{m s}^{-1}. \quad (6)$$

Here, it is noteworthy that the polarimetric measurements of C-band are not considered due to lack of available PGMF.

3 Simulation Experiments

An end-to-end simulation is carried out to analyze the wind retrieval of dual-frequency polarmetric scattreometer. The procedure starts with scanning geometry simulation, which incorporates the actual orbital parameters and the realistic earth rotation. Based on HY-2A/SCAT scanning geometry (Lin *et al.*, 2013), the dual-frequency polarimetric scatterometer is simulated with a scanning 'pencil-beam' antenna mode, which employs two pencil beams sweeping in a circular form. The incidence angles of inner and outer beams are 41° and 48°, respectively. The scanning geometry is shown in Fig.3.

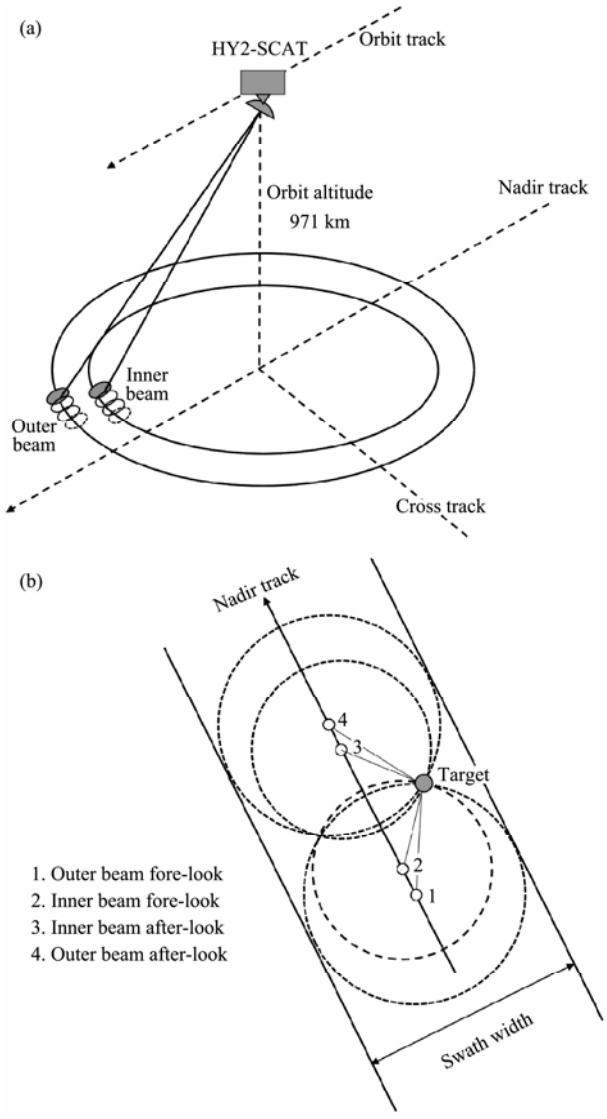

Fig.3 HY-2A/SCAT scanning geometry, (a) conically scanning geometry, (b) observation information.

The measured co- and cross-polirazied backscatter coefficients and the polarmetric backscatter coefficients (*i.e.*, σ_{VHHH} for the inner beam and σ_{HVVV} the outer beam) are simulated for 25 km WVCs through adding the random Gaussian noise to the backscatter coefficients computed by GMFs. The standard deviation of random noise is usually defined as the measured accuracy levels determined by the specified instrumental communication noise, the instrument calibration and model function errors. The communication noise is a function of signal-to-noise ratio and the number of independent measurements due to the measured energy fading and the thermal noise. The instrument calibration error is related to the internal calibration accuracy, the antenna gain and the accuracy of antenna pattern. The model error is caused by the inaccuracy of GMF varying with the wind speed and the observed spatial resolution. In order to analyze the difference between C-band and Ku-band scatterometers for retrieving wind vector with the same measured accuracy, the same standard deviations of random noises of dual-frequency co-polarized (or cross-polarized) backscatter coefficients are 0.7 (or 2.0), 0.63 (or 1.3), 0.55 (or 1.0) and 0.35 dB (or 0.6 dB) for the wind speeds of 5, 15, 25 and 45 m s^{-1}, respectively. Meanwhile, the relative errors of polarimetric backscatter coefficient are assumed to be about 60%, 20% , 18% and 16%, respectively.

To retrieve the wind vector, the retrieval algorithms of the wind vector and the wind direction ambiguity removing are needed (Martin, 2014). In this paper, the wind vector is estimated with Maximum Likelihood Estimation method and the circle median filter algorithm without external wind fields. The RMSE of the wind retrieval is determined by comparing the input wind vector used to simulate the measured backscatter coefficient with the retrieved wind field.

To test the capabilities of dual-frequency polarimetric measurement referencing the concept of HY-2A scatterometer, we operate two simulations. The first simulation is carried out for the following beam configurations, where inner beam and outer beam are designed for horizontal and vertical polarization, respectively.

A1. Ku-band HH on inner beam and VV on outer beam;

B1. C-band HH on inner beam and VV on outer beam;

C1. Ku-band HH, VHHH on inner beam and VV, HVVV on outer beam;

D1. C-band HH, VH on inner beam and VV, HV on outer beam;

E1. Ku-band HH and C-band HH on inner beam, Ku-band VV and C-band VV on outer beam.

F1. Ku-band HH, VHHH and C-band HH, VH on inner beam, Ku-band VV, HVVV and C-band VV, HV on outer beam;

The second simulation is the cases of replacing C-band vertical polarization with C-band horizontal polarization in outer beam,

A2. Ku-band HH on inner beam and VV on outer beam;

B2. C-band HH on inner beam and HH on outer beam;

C2. Ku-band HH, VHHH on inner beam and VV,

HVVV on outer beam;

D2. C-band HH, VH on inner beam and HH, VH on outer beam;

E2. Ku-band HH and C-band HH on inner beam, Ku-band VV and C-band HH on outer beam.

F2. Ku-band HH, VHHH and C-band HH, VH on inner beam, Ku-band VV, HVVV and C-band HH, VH on outer beam;

Note that the case A2 (or C2) and the case A1 (or C1) are the same. The Ku-band polarimetric measurements are not included in configuration C1, F1, C2 and F2 when the wind speed is larger than $25\,m\,s^{-1}$ owing to the unavailability of PGMFs for the high wind speed.

4 Simulation Results

4.1 First Simulation Results

Traditional conical scanning scatterometer of single-frequency and co-polarization has the disadvantage of large retrieval errors in nadir and outer swath because of the poor azimuth diversity. For evaluating the retrieval performance of dual-frequency polarimetric scatterometer across whole swath, Figs.4(a)–(f) show the wind retrieval RMSE varying with wind vector cell locations across the swath at wind speeds 5, 25 and $45\,m\,s^{-1}$, respectively. In Table 1, all of the retrieval RMSEs of wind speed and wind direction is listed for the wind speed range of 5 to $45\,m\,s^{-1}$.

These figures reveal that, within the nominal wind speed range ($Ws_{10} < 25\,m\,s^{-1}$), the retrieval error of conventional single-frequency measurement modes exhibits the obvious shape of 'w' due to the poor azimuth diversity in nadir and outer swath. The polarimetric measurements show the advantage over the conventional one for reducing the retrieval errors of wind direction in nadir and outer swath.

At low wind speed ($5\,m\,s^{-1}$), we find, from Figs.4(a), (b) and Table.1, that the dual-frequency measurement configuration E1 and F1 perform better than others because of more measurements available for retrieving wind vector, especially configuration F1 adds the polarimetric measurements on the basis of dual-frequency design. The co-polarized and polarimetric measurement configuration C1 of Ku-band also shows good retrieval results even though the measurement errors of polarimetric backscatter coefficient is large (60%) at low wind speed. In addition, it is seen that Ku-band configurations perform better than C-band at low wind speed.

At moderate and high wind speed (15 and $25\,m\,s^{-1}$), the absolute advantage of polarimetric measurements is evident. The different symmetry properties of the relative wind direction in the copolarization and polarimetric correlation signatures can improve the ability of resolving the wind direction ambiguity and generally enhance the overall wind retrieval accuracy across the measurement swath. As shown in Fig.4, compared to the results of Ku-band co-polarization mode A1(HY-2A/SCAT), the wind retrieval errors of polarimetric configurations C1 and F1 are greatly reduced, in particular the wind direction RMSE is reduced from 15° to 5°. Moreover, the comparison between the results of configuration B1 and D1 indicates that C-band cross-polarized measurements are of benefit to retrieving wind speed because of the high sensitivity of cross-polarized backscatter coefficient to the wind speed.

At extreme winds, the dual-frequency and the cross-polarized measurements are suitable to inverse the wind direction and the wind speed, respectively (Rivas *et al.*, 2014). As shown in Fig.4(h), the C-band configuration D1 incorporating cross-polarized measurements can enhance the wind speed accuracy about $2.3\,m\,s^{-1}$ comparing to the case B1. It is obvious that the case F1 having both dual-frequency and cross-polarized measurements is best for retrieving wind vector.

4.2 Second Simulation Results

Recently, the airborne experiment of C- and Ku-bands with HH and VV polarizations shows that the normalized radar cross sections (NRCS) are saturated with the wind speed increasing up to a certain high wind speed except for the large incidence angle of C-band and HH polarization (Fernandez *et al.*, 2006). This infers that the HH-polarized measurements of large incidence angles may be possible to improve the wind retrieval at high wind speed. One major innovation of the second-generation of meteorological satellite polar system (EPS-SG) with respect to ASCAT is the addition of horizontal copolarization at fore/aft beams to obtain better wind results at extreme winds (Stoffelen *et al.*, 2017). To discuss the effect of C-band HH-polarized measurements on retrieving the wind field, we conduct the second simulation by replacing the C-band V polarization measurement with C-band H polarization at outer beam, *i.e.*, the previously mentioned cases A2, B2, C2, D2, E2 and F2. The wind retrieval results at $45\,m\,s^{-1}$ are depicted in Fig.5. The retrieval RMSE results of all wind fields are listed in Table 2.

Table 1 Retrieval RMSE of wind speed and direction for the first simulation

Config	Wind speed retrieval RMSE ($m\,s^{-1}$)				Wind direction retrieval RMSE (°)			
	$5\,m\,s^{-1}$	$15\,m\,s^{-1}$	$25\,m\,s^{-1}$	$45\,m\,s^{-1}$	$5\,m\,s^{-1}$	$15\,m\,s^{-1}$	$25\,m\,s^{-1}$	$45\,m\,s^{-1}$
A1	0.30	1.43	2.25	3.44	17.11	15.69	17.51	28.94
B1	0.73	1.41	2.30	3.99	20.09	15.39	19.42	34.29
C1	0.33	1.09	1.92	/	12.11	5.15	5.17	/
D1	0.65	0.95	2.07	1.66	20.06	12.00	18.34	35.16
E1	0.21	1.10	1.85	3.05	11.56	12.05	14.42	24.37
F1	0.29	0.75	1.43	1.55	9.16	4.63	4.87	23.03

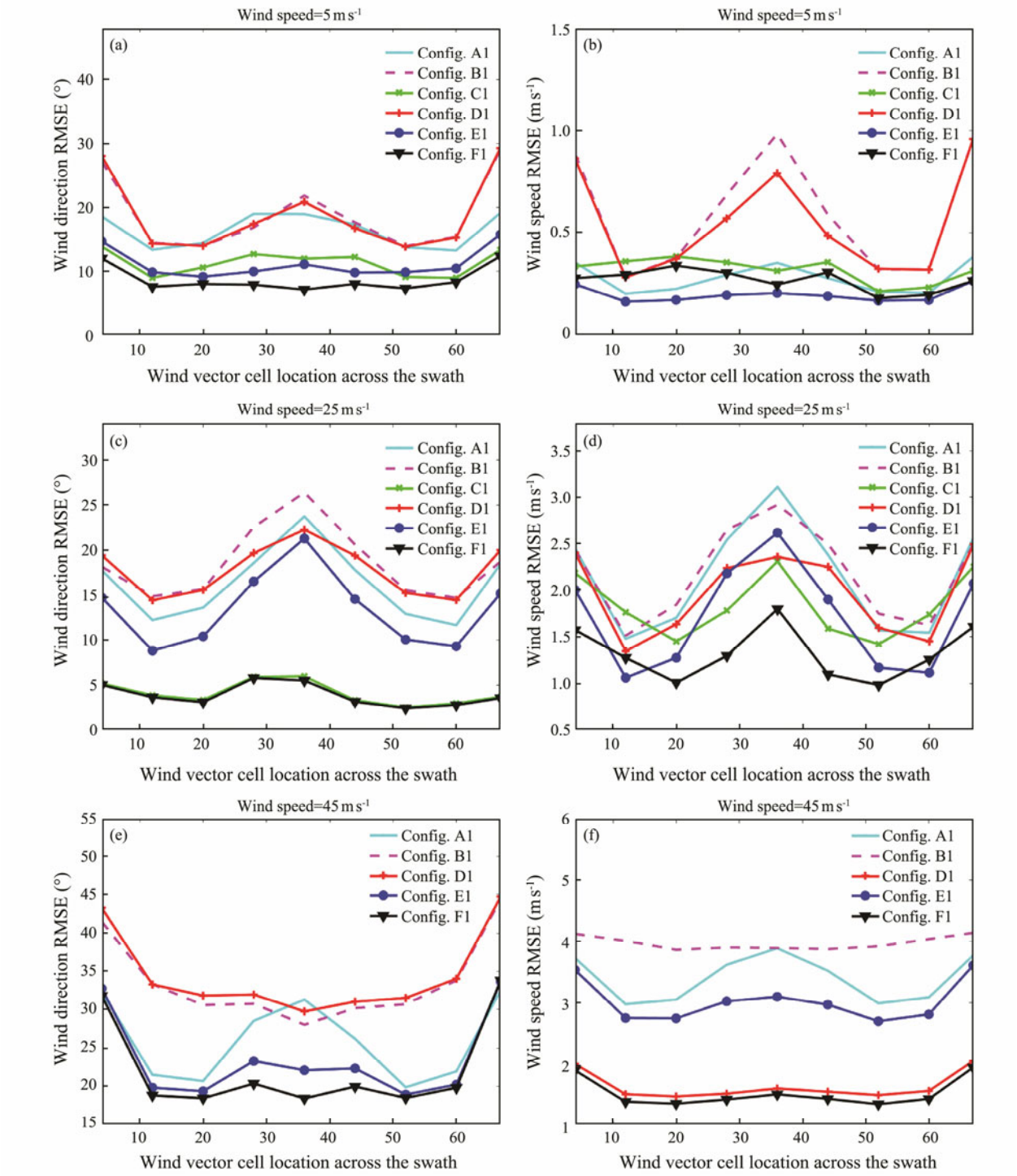

Fig.4 The variation of wind direction retrieval RMSE (left) and wind speed retrieval RMSE (right) *versus* WVC locations across the swath: (a) and (b) 5 m s^{-1}, (c) and (d) 25 m s^{-1}, (e) and (f) 45 m s^{-1}. It is noted that all configurations with H polarization at inner beam, and V polarization at outer beam.

Table 2 Retrieval RMSE of wind speed and direction for the second simulation

Config	Wind speed retrieval RMSE (m s^{-1})				Wind direction retrieval RMSE (°)			
	5 m s^{-1}	15 m s^{-1}	25 m s^{-1}	45 m s^{-1}	5 m s^{-1}	15 m s^{-1}	25 m s^{-1}	45 m s^{-1}
A2	0.30	1.39	2.25	3.42	17.01	15.62	17.11	28.59
B2	0.68	1.27	2.22	4.03	15.88	16.56	25.00	19.07
C2	0.33	1.09	1.92	/	11.94	5.04	5.19	/
D2	0.59	0.91	2.04	1.64	15.56	14.27	24.04	17.99
E2	0.20	1.05	1.70	2.85	9.80	12.70	14.78	15.11
F2	0.29	0.75	1.41	1.50	8.12	4.61	4.88	14.43

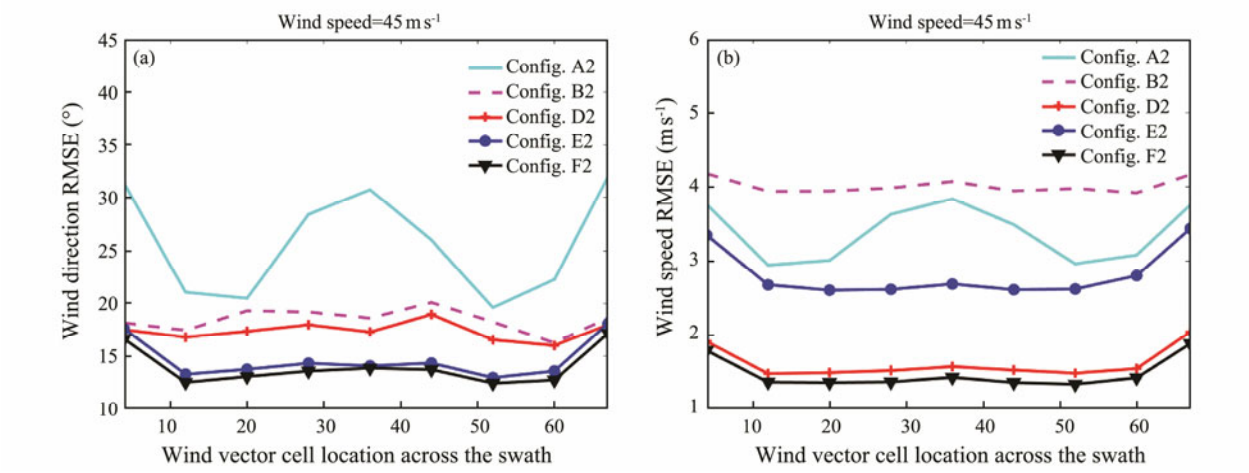

Fig.5 The variation of (a) wind direction retrieval RMSE and (b) wind speed retrieval RMSE versus with wind vector cell locations across the swath at the wind speed 45 m s^{-1}, where C-band V polarization is replaced by C-band H polarization at outer beam.

From Fig.4(g) and Fig.5(a), it is clear that the wind direction retrieval accuracy at 45 m s^{-1} is enhanced by using C-band H polarization to replace V polarization at outer beam (case B2, D2, E2, F2), with an improvement of about 9°. We find from Table 2 that, at extreme wind speed (45 m s^{-1}), the case F2 and D2 are valid for inversing the wind speed with RMSE about 1.6 m s^{-1}, and case E2 and F2 can be used to retrieve the wind direction with RMSE of about 15°. Generally, the case F2 is the best way for retrieving the sea surface wind vector having RMSE of the wind speed and the wind direction less than 1.5 m s^{-1} and 15°, respectively.

4.3 Results Analysis

As has been documented by the above simulation results, the conventional Ku-band scatterometer is not suitable for measuring the extreme winds. For the wind speed less than 25 m s^{-1}, the wind vector retrieval over the entire scatterometer swath can be improved dramatically by adding Ku-band polarimetric measurements. If we investigate the winds over hurricanes regions of extreme winds, the introduction of C-band measurements with horizontal polarization in both inner and outer beam is a desirable choice to enhance the wind vector retrieval, due to the unsaturation of HH polarization at extreme wind speed and the high sensitivity of VH to the wind speed. It has been clarified that the backscattered signals from the sea surface dominated by Bragg scattering usually are proportional to the density of surface elements with the ocean wavelengths of the order of centimeters. These ocean waves mainly respond to the strength of local winds. Thus, low microwave frequency, which interacts with long surface waves, has an advantage of measuring extreme winds. However, the high microwave frequency helps obtain the wind vector of low wind speeds. It is totally predictable that the combination of C-band and Ku-band, with addition of polarimetric capability, will acquire very good wind retrieval results for all wind conditions.

5 Conclusions

With the purpose of improving wind retrieval of HY-2A-type scatterometers for all winds speed (5–45 m s^{-1}), we constructed two wind retrieval simulations with some extensional measurements of dual-frequency and multi-polarization. The first simulation results indicate that polarimetric mesurments have an important potential of improving the wind vector retrieval for the wind speed less than 25 m s^{-1}, as well as for eliminating the disadvantage of conventional single-frequency and co-polarized scatterometer in nadir and outer swath. Moreover, it is expectable that the wind retrieval accuracy of dual-frequency measurement is better than that of single frequency for all wind speeds because of more measurements used in retrieving wind vector. The dual-frequency and polarimetric configurations are best for retrieving the low-to-high wind speed with the wind direction RMSEs of 9.2, 4.6, 4.9° and the wind speed RMSEs of 0.3, 0.8, 1.4 m s^{-1} for wind speed 5, 15 and 25 m s^{-1}, respectively.

The difference between the second simulation and the first one is that C-band VV polarization at outer beam is replaced by HH polarization. The new simulation reveals that, at 45 m s^{-1}, the C-band HH polarization offers an improved wind direction RMSE of 14.4° (comparing RMSE 23.0° for the C-band VV options) over the entire swath. On the other hand, the cross-polarized measurements results in the retrieved wind speed with RMSE of 1.5 m s^{-1}. For low-to-high wind speed (5–25 m s^{-1}), the C-band HH polarization provides almost the same retrieval results as that of VV polarization.

In summary, dual-frequency polarimetric scatterometer, which incorporates Ku-band and C-band H polarization at inner beam, and Ku-band V polarization and C-band H polarization at outer beam, is valid to retrieve more accurate ocean wind vector for both low and high wind speed (5–45 m s^{-1}). To accurately estimate the wind fields, it is necessary to study the polarimetric backscatter coefficient under high wind speeds so that one can develop a mature

polarimetric GMF.

Acknowledgements

The study was supported by the National Key R&D Program of China (No. 2016YFC1401006), the National Natural Science Foundation of China (Nos. 51279186, 51479183 and 41676169), the National Program on Key Basic Research Project (No. 2011CB013704), the 111 Project (No. B14028), and the Marine and Fishery Information Center Project of Jiangsu Province (No. SJC2014 110338).

References

Carswell, J. R., Carson, S. C., McIntosh, R. E., Li, F. K., Neumann, G., McLaughlin, D. G.,Wilkerson, J. C., Black, P. G., and Nghiem, S. V., 1994. Airborne scatterometers: Investigating ocean backscatter under low- and high-wind conditions. *Proceeding of the IEEE*, **82** (12): 1835-1860.

Chelton, D. B., and Xie, S. P., 2010. Coupled ocean-atmosphere interaction at oceanic mesoscales. *Oceanography*, **23** (4): 52-69.

Chiara, G. D., 2017. Improving the assimilation of scatterometer wind observations in global NWP. *IEEE Journal of Selected Topics in Applied Earth Observations and Remote Sensing*, **PP** (99): 1-9.

Durden, S. L., and Perkovic-Martin, D., 2017. The RapidScat Ocean winds scatterometer: A radar system engineering perspective. *IEEE Geoscience and Remote Sensing Magazine*, **5** (3): 36-43.

Fernandez, D. E., Carswell, J. R., Frasier, S., Chang, P. S., Black, P. G., and Marks, F. D., 2006. Dual-polarized C- and Ku-band ocean backscatter response to hurricane-force winds. *Journal of Geophysical Research*, **111**: C08013.

Figa-Saldana, J., Wilson, J. J. W., Attema, E., Gelsthorpe, R., Drinkwater, M. R., and Stoffenlen, A., 2002. The Advanced Scatterometer (ASCAT) on the meteorological operational (MetOp) platform: A follow on for European wind scatterometers. *Canadian Journal of Remote Sensing*, **28** (3): 404-412.

Freilich, M. H., and Dunbar, R. S., 1999. The accuracy of the NSCAT-1 vector winds: Comparisons with national data buoy center buoys. *Journal of Physical Research*, **104** (C5): 11231-11246.

Freilich, M. H., and Wentz, F., 1997. Finalizing the NSCAT-1 model and progress towards NSCAT-2. *Proceeding of NASA Scatterometer Science Symposium*. Hawaii, 146-148.

Freilich, M. H., Long, D. G., and Spencer, M. W., 1994. SeaWinds: A scanning scatterometer for ADEOS-II-science overview. *Proceedings of the 1994 International Geoscience and Remote Sensing Symposium on Surface and Atmospheric Remote Sensing: Technologies, Data Analysis and Interpretation*, **2**: 960-963.

Gaston, R., and Rodriguez, E., 2008. Quikscat follow-on concept study report. Technical Report. Jet Propulsion Laboratory. Pasadena, California, 08-18.

Graf, J. E., Naderi, F., and Tsai, W. Y., 1995. Overview of NASA scatterometers projects. *Proceedings of the 1995 International Geoscience and Remote Sensing Symposium on Quantitative Remote Sensing for Science and Applications*, **2**: 1564-1566.

Hersbach, H., 2008. CMOD5.n: A C-band geophysical model function for equivalent neutral wind. *ECMWF Technical Memorandum*, No.554, 22pp.

Hwang, P. A., Zhang, B., Toporkov, J. V., and Perroe, W., 2010. Comparison of composite Bragg theory and quad-polarization radar backscatter from RADARSAT-2: With applications to wave breaking and high wind retrieval. *Journal of Geophysical Research*, **115** (C8): C08019-12.

Jayaram, C., Bhaskar, U., Swain, D., and Bansal, S., 2017. Oceansat-2 Scatterometer (OSCAT) wind fields over the global oceans. *Proceedings of the National Academy of Science, India Section A: Physical Sciences*, **87** (4): 797-806.

Kasaka, Y., 2014. Increasing wind sinks heat. *Nature Climate Change*, **4**: 172-173.

Lin, M. S., and Zou, J. H., 2013. HY-2A microwave scatterometer wind retrieval algorithm. *Engineering Sciences*, **15** (7): 70-76.

Lin, W. M., Portabella, M., Stoffelen, A., and Verhoef, A., 2017. Toward an improved wind inversion algorithm for RapidScat. *IEEE Journal of Selected Topics in Applied Earth Observations and Remote Sensing*, **10** (5): 2156-2164.

Linwood-Jones, W., Schroeder, L. C., Bracalente, E. M., Boggs, E. M., Brown, R. A., Dome, G. J., Pierson, W. J., and Wentz, F. J., 1982. The Seasat-A satellite scatterometer: The geophysical evaluation remote sensed winds over the ocean. *Journal of Geophysical Research*, **87**: 3297-3317.

Martin, S., 2014. *An Introduction to Ocean Remote Sensing*. Cambridge University Press, Cambridge, 476pp.

Moore, R. K., and Fung, A. K., 1997. Radar determination of winds at sea. *Proceeding of the IEEE*, **67** (11): 1504-1521.

Nghiem, S. V., Li, F. K., and Neumann, G., 1996. Ku-band ocean backscatter functions for surface wind retrieval. *Proceeding of the 1996 International Geoscience and Remote Sensing Symposium on Remote Sensing for a Sustainable Future*, **3**: 1469-1471.

Nghiem, S. V., Li. F. K., Lou, S. H., Neumann. G., McIntosh, R. E., Carson, S. C., Carswell, J., Walsh, E., Donelan, M. A., and Drennan, W., 1995. Observations of ocean radar backscatter at Ku and C bands in the presence of large waves during the surface wave dynamics experiment. *IEEE Transaction on Geoscience and Remote Sensing*, **33**(3): 708-721.

Rivas, M. B., Stoffelen, A., and Zadelhoff, G. J., 2012. Polarization options for the EPS-SG scatterometer. *NWP/SAF Associate Scientist Mission Report*. NWPSAF-KN-VS-009.

Rivas, M. B., Stoffelen, A., and Zadelhoff, G. J., 2014. The benefit of HH and VH polarizations in retrieving extreme wind speeds for an ASCAT-Type scatterometer. *IEEE Transaction on Geoscience and Remote Sensing*, **52** (7): 4273-4280.

Rodriguez, E., Gaston, R. W., Durden, S. L., Stiles, B., Spencer, M., Veilleus, L., Hughes, R., Fernadez, D. E., Chan, S., Veleva, S., Dunbar, R. S., 2009. A scatterometer for XOVWM, the extended ocean vector winds mission. *IEEE National Radar Conference*. Pasadena, California, 1-4.

Schultz, H., 1990. A circular median filter approach for resolving directional ambiguities in wind fields retrieved from spaceborne scatterometer data. *Journal of Geophysical Research*, **95** (4): 5291-5303.

Soisuvarn, S., Jelenak, Z., Chang, P. S., Alsweiss, S. O., and Zhu, Q., 2013. CMOD5.H–A high wind geophysical model function for C-band vertical polarized satellite scatterometer measurements. *IEEE Transaction on Geoscience and Remote Sensing*, **51** (6): 3744-3760.

Soisuvarn, S., Jelenak, Z., Chang, P. S., Zhu, Q., and Sindic-Rancic, G., 2008. Validation of NOAA's near real-time ASCAT ocean vector winds. *IEEE International Geoscience and Remote Sensing Symposium*. Boston, Massachusetts, I118-I121.

Spencer, M. W., Wu, C., and Long, D. G., 1997. Tradeoffs in the

design of a spaceborne scanning pencil beam scatterometer: Application to Sea-Winds. *IEEE Transaction on Geoscience and Remote Sensing*, **35** (1): 115-126.

Stoffelen, A., Aaboe, S., Calvet, J.-C., Cotton, J., Chiara, G. D., Saldana, J. F., Mouche, A. A., Portabella, M., Scipal, K., and Wolfgang, W., 2017. Scientific developments and the EPS-SG scatterometer. *IEEE Journal of Selected Topics in Applied Earth Observations and Remote Sensing*, **10** (5): 2086-2097.

Stoffelen, A., and Portabella, M., 2006. On Bayesian scatterometer wind inversion. *IEEE Transaction on Geoscience and Remote Sensing*, **44** (6): 1523-1533.

Tsai, W. Y., Nghiem, S. V., Huddleston, J. N., Spencer, M. W., Stiles, B. W., and West, R. D., 2000. Polarimetric scatterometer: A promising technique for improving ocean surface wind measurements from space. *IEEE Transaction on Geoscience and Remote Sensing*, **38** (4): 1903-1921.

Vachon, P. W., and Wolfe, J., 2011. C-band cross-polarization wind speed retrieval. *IEEE Geoscience and Remote Sensing Letters*, **8** (3): 456-459.

Verspeek, J., Stoffelen, A., Portabella, M., Bonekam, H., Anderson, C., and Figa-Saldana, J., 2010. Validation and calibration of ASCAT using CMOD5.n. *IEEE Transaction on Geoscience and Remote Sensing*, **48** (1): 386-395.

Wentz, F. J., and Ricciardulli, L., 2011. Comment on 'Global trends in wind speed and wave height'. *Science*, **334** (5058): 905.

Wentz, F. J., and Smith, D. K., 1999. A model function for the ocean normalized cross section at 14 GHz derived from NSCAT observation. *Journal of Geophysical Research*, **104** (C5): 11499-11507.

Wentz, F. J., Freilich, M. H., and Smith, D. K., 1998. NSCAT-2 geophysical model function. *Proceeding of AGU Fall Meeting on Ocean Science*. San Diego, California, **OS72G-01**: 1-10.

Yueh, S. H., 1997. Modeling of wind direction signals in polarimetric sea surface brightness temperatures. *IEEE Transaction on Geoscience and remote sensing*, **35** (6): 1400-1418.

Yueh, S. H., Kwok, R., and Nghiem, S. V., 1994. Polarimetric scattering and emission properties of targets with reflections symmetry. *Radio Science*, **29** (6): 1409-1420.

Yueh, S. H., Stiles, B. W., Tsai, W. Y., Hu, H., and Liu, W. T., 2001. Quikscat geophysical model function for tropical cyclones and application to hurricane floyd. *IEEE Transaction on Geoscience and Remote Sensing*, **3 9**(12): 2601-2612.

Yueh, S. H., Wilson, W. J., and Dinardo, S., 2002. Polarimetric radar remote sensing of ocean surface wind. *IEEE Transaction on Geoscience and Remote Sensing*, **40** (4): 793-800.

(Edited by Xie Jun)